ORIGINAL PAPER

Pulsating instabilities in the Zeldovich–Liñán model

**V. V. Gubernov · A. V. Kolobov · A. A. Polezhaev ·
H. S. Sidhu**

Abstract   In this paper we numerically study the properties and stability of the travelling combustion waves in Zeldovich–Liñán model in the adiabatic limit in one spatial dimension. The structure and the properties of the combustion waves are found to depend on the recombination parameter, showing the relation between the characteristic times of the branching and recombination reactions. For small (large) values of this parameter the slow (fast) recombination regime of flame propagation is observed. The dependence of flame speed on the parameters of the model are studied in detail. It is found that the flame speed is unique, the combustion wave does not exhibit extinction as the activation energy is increased. The flame speed is a monotonically decreasing function of the activation energy. The results are compared to the prediction of the activation energy asymptotic analysis. It is found that the correspondence is good for the fast recombination regime and large activation energies. Stability of combustion waves is studied by using the Evans function method and direct integration of the governing partial differential equations. It is demonstrated that the combustion waves lose stability due to supercritical Hopf bifurcation. The neutral stability boundary is found in the space of parameters. The pulsating solutions emerging as a result of Hopf bifurcation are investigated. The amplitude of pulsations grow in a root type manner as the activation energy is increased beyond the neutral stability boundary.

V. V. Gubernov (✉) · A. V. Kolobov · A. A. Polezhaev
I.E. Tamm Theory Department, P.N. Lebedev Physical Institute of Russian Academy of Sciences,
53, Leninskii prospect, Moscow 119991, Russian Federation
e-mail: gubernov@lpi.ru; vvg@spmlab.phys.msu.su

H. S. Sidhu
School of Physical, Environmental and Mathematical Sciences,
University of New South Wales at the Australian Defence Force Academy,
Canberra, ACT 2600, Australia

1 Introduction

Most of the flames proceed via complex multi-step reaction mechanisms. Important in terms of practical applications hydrocarbon-air and hydrogen-air flames are usually modelled with chain-branching reaction kinetics. Such flames normally produce a pool of radicals through the branching reaction steps. These radicals later recombine to produce heat and products. The chain-branching reaction mechanism cannot be adequately described by an overall single reaction and in the most basic case at least two-step kinetic mechanisms are required to model it, whereas the detailed kinetic schemes for hydrocarbon-air and hydrogen-air flames include dozens or hundreds of reaction steps.

The first two-step chain branching reaction model was introduced by Zeldovich in 1948 [1], where the model equations were set up. Later the model was analyzed by Liñán [2] using the activation energy asymptotics (AEA). Therefore this model is usually referred to as the Zeldovich–Liñán model. The model comprises a chain branching reaction $A + B \rightarrow 2B$, and a chain-breaking (or recombination) reaction $B + B + M \rightarrow 2P + M$, where A is the fuel, B is the intermediate radical, P is the product, and M is a third body of collision needed for recombination, which is not changed by the reaction. It is assumed that the first reaction has a large activation energy and is isothermic (zero heat release) whereas, the recombination reaction has zero activation energy and is exothermic. The condition of an isothermic first reaction was subsequently relaxed in [3].

In [2] it was shown that there are three flame regimes in the Zeldovich–Liñán model: fast, slow and intermediate recombination. In the fast recombination regime the production of radicals by the branching step is much slower than the consumption of radicals through the recombination step. This has the following consequences: chain-branching and chain-recombination take place in the same thin reaction zone, the concentration of radicals is asymptotically small, and therefore the steady state approximation can be applied to it. In the slow recombination regime, the concentration of radicals is of the order of unity and all radicals are produced in a thin reaction zone. However, the consumption of radicals proceeds in a long scale region greater or comparable to the convection-diffusion region. In the intermediate recombination regime, the rates of the branching and termination reactions are comparable. The concentration of radicals is of the order of the dimensionless burned temperature and the recombination reaction takes place in a region, which is much thicker than the branching reaction zone, but much thinner than the convection-diffusion region.

Using the above arguments, various asymptotic expansions have been introduced in different flame zones. The resulting asymptotic differential equations are then solved either symbolically or numerically depending on the complexity of the system of equations appearing as a result of asymptotic analysis. The model considered in [2,3] does not include heat loss and the response curves obtained in these papers are single valued functions. In [4] the Zeldovich–Liñán model with heat loss to the surroundings was considered by using the AEA. It was demonstrated that the flame speed as a function

of other parameters of the problem is a C-shaped function which exhibits turning point-type extinction condition similar to that predicted by the one-step nonadiabatic model [5].

In a number of investigations [6–9], the influence of stretch on premixed flame for the Zeldovich–Liñán model was studied. The authors considered several distinguished limits in order to examine the problem in terms of AEA either analytically or semi-analytically. As a result it was found that the flame response to stretching depended upon the particular flame regime i.e. slow, fast or intermediate recombination.

In [10], a slightly modified model with the first reaction of the form $A + B \rightarrow 3B$ was used to describe the hydrogen-oxygen flame. Approximate formulas for the deflagration speed were obtained in the limits of strong and weak recombination. Recently [11,12] these results were tested using the numerical calculations with the detailed mechanism of the reaction and it was demonstrated that the two-step reaction model gives a good approximation of the flame propagation velocity.

Despite the apparent success in the investigation of the speed of the combustion waves, the stability of flames in the Zeldovich–Liñán model has not been investigated. A simplified version of the Zeldovich–Liñán model with the first order recombination reaction was introduced recently [13], where the properties and stability of the travelling combustion waves were studied using AEA. In our recent papers [14–16] we numerically investigated the properties of travelling combustion waves and their stability with respect to pulsating perturbations and compared the results with the predictions from the corresponding one-step models and the results presented in [13]. However the kinetics can change the properties of combustion waves significantly and the results obtained for the model introduced in [13] cannot be directly applied to the Zeldovich–Liñán model. The aim of our current paper is to investigate the stability of combustion waves in the Zeldovich–Liñán model with respect to pulsating perturbations.

The paper is organized as follows. In Sect. 2 the governing equations and boundary conditions for the model are introduced in both dimensional and dimensionless forms. In Sect. 3 the properties of the travelling combustion waves are studied in detail and the linear stability analysis of these solutions is carried out in Sect. 4. In Sect. 5 the pulsating solutions emerging as the neutral stability boundary is crossed in the space of parameters are investigated. The conclusions are presented in Sect. 6.

2 Model

We consider a diffusional thermal adiabatic model (in one spatial dimension) that includes two steps: autocatalytic chain branching $A + B \rightarrow 2B$ and recombination $B + B + M \rightarrow 2P + M$. Following the approach of [1] it is assumed that all the heat of the reaction is released during the recombination stage and the chain branching stage does not produce or consume any heat. According to [4], the dimensional equations governing this process can be written as

$$\rho c_p \frac{\partial T}{\partial t} = \lambda \frac{\partial^2 T}{\partial x^2} + q_F W_A A_R \left(\frac{\rho Y_B}{W_B} \right)^2 \frac{\rho Y_M}{W_M},$$

$$\rho \frac{\partial Y_A}{\partial t} = \rho D_A \frac{\partial^2 Y_A}{\partial x^2} - A_B \frac{\rho Y_A}{W_A} \frac{\rho Y_B}{W_B} e^{-E/RT},$$

$$\rho \frac{\partial Y_B}{\partial t} = \rho D_B \frac{\partial^2 Y_B}{\partial x^2} + W_B \left(A_B \frac{\rho Y_A}{W_A} \frac{\rho Y_B}{W_B} e^{-E/RT} - 2A_R \left(\frac{\rho Y_B}{W_B} \right)^2 \frac{\rho Y_M}{W_M} \right), \quad (1)$$

where T is the temperature; Y_A and Y_B represent the mass fraction of fuel and radicals respectively; ρ is the density; λ is the thermal conductivity; c_p is the specific heat; D_A and D_B represent the diffusivity of fuel and radicals respectively, A_R and A_B are constants of recombination and chain branching reactions respectively; W_A, W_B, and W_M represent the molecular weight of fuel, radicals and a third body; q_F is the specific heat of the recombination reaction; E is the activation energy for chain branching reaction; R is the universal gas constant. Equation (1) are considered subject to boundary conditions

$$\begin{array}{llll} T = T_a, & Y_A = Y_A^\infty, & Y_B = 0 & \text{for } x \to +\infty, \\ dT/dx = 0, & dY_A/dx = 0, & dY_B/dx = 0 & \text{for } x \to -\infty, \end{array} \quad (2)$$

which correspond to a wave travelling in the positive x direction. Upstream, on the right boundary, T is equal to the ambient temperature, T_a; fuel has not been consumed yet and Y_A is equal to its maximal initial value in the cold unreacted mixture, Y_A^∞; no radicals have been produced i.e. $Y_B = 0$. Downstream, on the left boundary, we require that there is no reaction happening, so the solution reaches a stationary point of (1). Therefore the zero flux conditions are taken for T, Y_A, and Y_B.

Introducing the nondimensional variables

$$t' = \frac{\rho A_B}{\beta M^*} t, \quad x' = \sqrt{\frac{\rho^2 A_B c_p}{\lambda M^* \beta}} x, \quad u = \frac{T}{T^* \beta}, \quad v = \frac{Y_A}{Y_A^\infty}, \quad w = \frac{Y_B W_A}{Y_A^\infty W_B}, \quad (3)$$

and dimensionless parameters

$$M^* = \frac{W_A}{Y_A^\infty}, \quad T^* = \frac{q_F Y_A^\infty}{2 c_p} x, \quad \beta = \frac{2 E c_p}{R q_F Y_A^\infty}, \quad L_{A,B} = \frac{\lambda}{D_{A,B} \rho c_p}, \quad r = \frac{2 A_R Y_M \rho M^* Y_A^\infty}{A_B W_M W_A}, \quad (4)$$

where M^* and T^* is the reference mass and temperature respectively, β is the dimensionless activation energy, L_A and L_B are the Lewis numbers for fuel and radicals respectively, we write (1) and (2) omitting primes as

$$\begin{aligned} u_t &= u_{xx} + r w^2, \\ v_t &= L_A^{-1} v_{xx} - \beta v w e^{-1/u}, \\ w_t &= L_B^{-1} w_{xx} + \beta v w e^{-1/u} - r \beta w^2, \end{aligned} \quad (5)$$

and

$$\begin{array}{llll} u = u_a, & v = 1, & w = 0 & \text{for } x \to \infty, \\ u_x = 0, & v_x = 0, & w_x = 0 & \text{for } x \to -\infty. \end{array} \quad (6)$$

The requirement that the reaction is frozen up- and downstream (i.e. the equilibrium is reached for the Eq. (5) in both limits $x \to \pm\infty$) from the reaction zone has the following implications. The right boundary condition is a stable equilibrium. Therefore small fluctuations of radical concentration should relax to $w = 0$, which implies that the branching term in (5) should vanish. It is possible only if the Arrhenius term is equal to zero i.e. $e^{-1/u_a} = 0$. Thus we encounter the 'cold boundary problem' for this model. In order to circumvent this issue, we consider zero temperature boundary condition $u_a = 0$, which is a standard technique for the one-step models [17]. In the opposite limit $x \to -\infty$, the boundary values for temperature and species concentration are undefined. Nevertheless, since it is assumed that the reaction is frozen downstream of the reaction front, the source terms in the right hand sides of Eq. (5) must vanish. It follows from the first equation in (5), that $w = 0$ on the right boundary. We refer the reader to [18] for more formal discussion on well-posedness of the problem of combustion waves propagation in models with complex kinetics.

3 Travelling wave solution

The solution to the problem (5), (6) is sought in the form of a traveling wave $u(x, t) = u(\xi)$, $v(x, t) = v(\xi)$, and $w(x, t) = w(\xi)$, where a coordinate in the moving frame, $\xi = x - ct$, is introduced and c is the speed of the traveling wave. Substituting the solution of this form into the governing equations we obtain

$$
\begin{aligned}
&u_{\xi\xi} + cu_\xi + rw^2 = 0, \\
&L_A^{-1}v_{\xi\xi} + cv_\xi - \beta vwe^{-1/u} = 0, \\
&L_B^{-1}w_{\xi\xi} + cw_\xi + \beta vwe^{-1/u} - r\beta w^2 = 0.
\end{aligned}
\tag{7}
$$

The boundary conditions (6) can be modified if we multiply the first equation in (7) by β, add it to the second and third equations in (7) and integrate it once with respect to ξ over $(-\infty, +\infty)$. This yields a condition: $\lim_{\xi\to-\infty} S = \lim_{\xi\to+\infty} S$, where $S = \beta u + v + w$. Combining this condition with (6) results in

$$
\begin{aligned}
u = 0, & \quad v = 1, \ w = 0 \ \text{for} \ \xi \to \infty, \\
u = \beta^{-1}(1 - \sigma), & \quad v = \sigma, \ w = 0 \ \text{for} \ \xi \to -\infty,
\end{aligned}
\tag{8}
$$

where σ denotes the residual amount of fuel left behind the wave and is unknown until a solution is obtained.

In the phase space of dynamical system (7) the travelling wave solution corresponds to a trajectory connecting two fixed points of Eq. (7). If a vector with coordinates $\mathbf{v} = (u, u_\xi, v, v_\xi, w, w_\xi)$ is introduced then the fixed points are $S_1 : \mathbf{v} = (0, 0, 1, 0, 0, 0)$ and $S_2 : \mathbf{v} = (\beta^{-1}(1 - \sigma), 0, \sigma, 0, 0, 0)$. If the system of Eq. (7) is linearized near $S_{1,2}$ and the Ansatz $\mathbf{v}(\xi) = \mathbf{k}\exp(\mu\xi)$ is used, it is easy to obtain the eigenvalues $\mu^{(1,2)}$ and corresponding eigenvectors $\mathbf{k}^{(1,2)}$ of the resulting algebraic system of equations. For the upstream fixed point, S_1, the spectrum of eigenvalues is $\mu^{(1)} = -c, -cL_A, -cL_B$ and triple degenerate $\mu^{(1)} = 0$, therefore S_1 is either stable or neutral along the corresponding eigenvectors. In the opposite limit, S_2, the

spectrum of eigenvalues can be found as $\mu^{(2)} = -c, -cL_A$, double degenerate 0, and $L_B^{-1}\left(-c \pm \sqrt{c^2 - 4\beta\sigma L_B^{-1} e^{-\beta/(1-\sigma)}}\right)/2$ which are both negative. So, the downstream fixed point S_2 is also either stable or neutral along the corresponding eigenvectors. Judging from the linear stability analysis we conclude that there cannot exist a trajectory in the phase space which connects S_1 and S_2, since there can be a trajectory converging to S_1, however no trajectory can depart from S_2 in this case. However, due to the presence of neutral eigenvalues and eigenvectors, in the nonlinear approximation there can exist a trajectory originating from S_2 along these neutral eigenvectors and thus connecting S_1 and S_2 in the phase space. Therefore, with the use of nonlinear analysis only the asymptotic behaviour of the solution to (7) in the limit $\xi \to -\infty$ can be found.

In the appendix, the leading order asymptotic behaviour of the solution of (7) in the limit $\xi \to -\infty$ is given. It is shown that there is no fuel leakage in the model i.e. $\sigma = 0$ and the value of temperature on the left boundary is therefore $u = \beta^{-1}$. The relation (18) between the values of dynamical variables are found. It is seen that there are two different regimes of flame propagation depending on the value of parameter $R = re^\beta$, which characterizes the ratio of the reaction rates of branching and recombination. If $R \ll 1$, then the branching reaction is faster than the recombination reaction and we have the slow recombination regime and vice versa, if $R \gg 1$ the fast recombination regime is encountered. Equations (7) and (18) together with the boundary conditions obtained from the linear asymptotic analysis in the limit $\xi \to +\infty$, namely, $cu + u_\xi = 0$, $c(v-1) + L_A v_\xi = 0$, and $cw + L_B w_\xi = 0$, constitute the two-point boundary value problem, which is solved numerically by using a standard shooting algorithm with a fourth order Runge–Kutta integration scheme first and then the results are corrected by employing the relaxation algorithm.

In Fig. 1 the characteristic solution profiles $u(\xi)$, $v(\xi)$, and $w(\xi)$ are plotted for two regimes of flame propagation i.e. the fast recombination, $r = 100$, curves 1 and the slow recombination, $r = 0.01$, curves 2. The other parameters are taken as shown in the figure caption. The graphs are scaled so that ξ changes from 0 to 1 and the profiles for $r = 100.0$ and $r = 0.01$ can be plotted in the same figures. For profiles 1 the length of the domain of integration is 2.6×10^3 and for profiles 2 it is 870. In Fig. 1b the radical concentration profiles are plotted in logarithmic scale since the maximum values of w for curves 1 and 2 varies in several orders of magnitude and cannot be presented in linear scale on the same graph. As seen in figure (b) the slow recombination regime (curve 2) is characterized by relatively large peak values of radical concentration, $\max w \sim O(1)$. The upstream form of $\log w(\xi)$ is linear indicating that the governing process here is the diffusion of radicals and heat from the hot reaction zone. This part of the solution is well described by the linear asymptotic analysis of (7) near S_2. In the product region, behind the reaction zone, the radicals are slowly consumed due to the recombination reaction and the $w(\xi)$ dependence is sub-exponential. The temperature profile $u(\xi)$ in figure (a) exhibits slow convergence to asymptotic value $u = 1$ in the product region as well. In contrast, $v(\xi)$ is similar to a step function with a narrow branching reaction zone where almost all fuel is consumed and v switches from maximal to minimal values. In other words, in the regime shown with curves 2 in Fig. 1, the large amount of radicals is produced in the thin
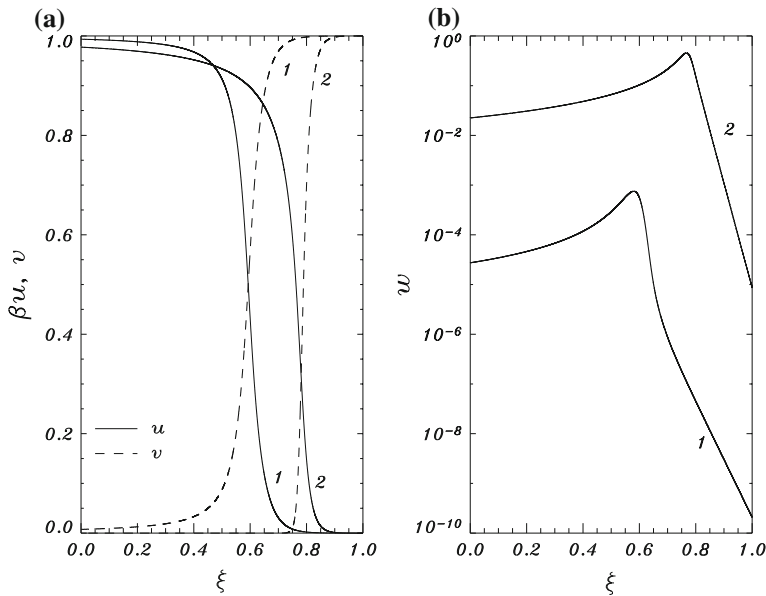
Fig. 1 Temperature $u(\xi)$, fuel concentration $v(\xi)$ profiles in (**a**) and radical concentration profile $w(\xi)$ in (**b**) for $L_A = L_B = 1$, $\beta = 1$, and two values of r. In (**a**) the *solid line* corresponds to $u(\xi)$ and the *dashed line* to $v(\xi)$. Curves 1 and 2 show the profiles for $r = 100$ and 0.01, respectively. Graph (**b**) is plotted in logarithmic scale

branching reaction zone which consumes almost all fuel. The radical concentration, $w(\xi)$, reaches its peak value, which is then followed by a gradual decay of $w(\xi)$ and rise of $u(\xi)$ due to the slow recombination reaction in the much wider recombination zone. For the fast recombination regime shown with curves 1, the maximum value of w is much smaller and is of the order of 10^{-3}. The radical concentration profile is more localized near its peak value. The region where the diffusion is the dominating process and $\log w(\xi)$ dependence is linear is followed by a rapid growth of the radical concentration closer to the maximum of $w(\xi)$. This is where the branching reaction becomes the governing process and the fuel depletion begins. Comparing the profiles of $v(\xi)$ and $w(\xi)$ in Fig. 1a and b we conclude that the recombination reaction, where most of the radicals are localized, occurs in a thinner zone, than the branching reaction region, where most of the fuel is consumed. In the product region, behind the reaction zone, $w(\xi)$ dependence is sub-exponential indicating that the reactions are still taking place here and the dynamics of (7) is nonlinear. This picture of various regimes of combustion wave propagation qualitatively agree with the results of [2].

In Fig. 2a the dependence of the speed c on β is plotted for different values of r : 0.01 curve 1, 1.0 curve 2, 100.0 curve 3. The results of numerical integration are shown with the solid line. The flame speed is presented in logarithmic scale to reveal various regimes of combustion wave propagation. The cross symbol located on curve 1 indicates the parameter values where $R = re^{\beta} = 1$ for $r = 0.01$. To the right from the cross, R becomes larger than unity and the fast recombination regime is encountered. As seen in Fig. 2a for $R > 1$ the $\log c(\beta)$ becomes almost linear function.
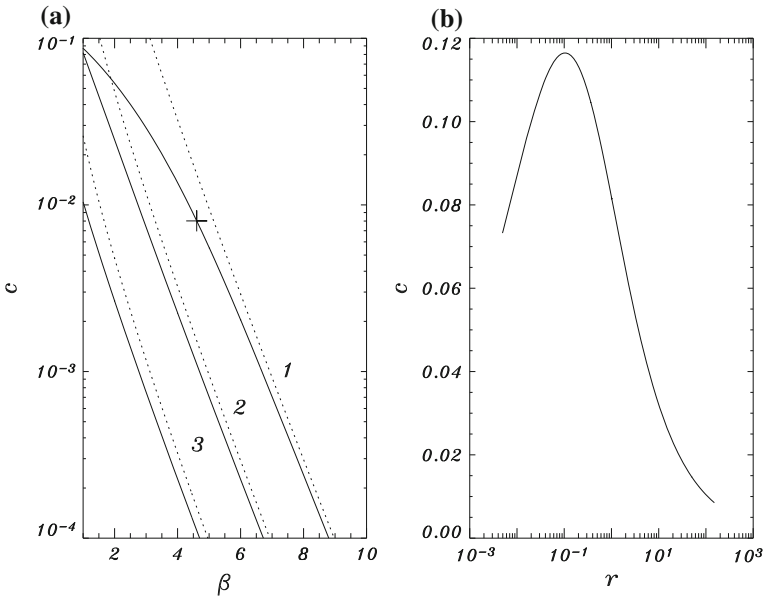
Fig. 2 The dependence of combustion wave speed, c, on β in (**a**) and c on r in (**b**) for $L_A = L_B = 1$. In (**a**) speed is plotted in logarithmic scale, the *solid line* represents the results of numerical analysis and the *dotted line* is the prediction of AEA. The value of r is equal to 0.01 for curve 1, 1.0 for curve 2, and 100.0 for curve 3. In figure (**b**) parameter r is plotted in logarithmic scale and $\beta = 1.0$

In contrast to that, to the left from the cross, where $R < 1$ curve 1 substantially departs from the linear behaviour. For curves 2 and 3 with larger values of r the point where $R = 1$ moves to much smaller β values and is not shown here, consequently, the fast recombination regime occurs in the whole range of activation energies shown in Fig. 2a and the dependence of $\log c$ on β is almost linear. In [2] it is shown that in the limit of fast recombination regime the quasi-steady state approximation applies for the radical species and the two-step chain-branching model can be reduced to the one-step model with the second-order reaction and double the activation energy of the branching reaction. The flame speed is found then using the AEA in the first order of asymptotic expansion for the case of $L_A = L_B = 1$. In [4] the analysis is generalized for the case of arbitrary Lewis numbers for fuel and radicals in both adiabatic and non-adiabatic cases. Converting these results to the current nondimensionalization yields the following expression for the flame speed

$$c = \frac{L_A e^{-\beta}}{\beta\sqrt{2r}}. \tag{9}$$

The dotted lines in Fig. 2a represent the prediction of the AEA according to formula (9). It is seen that in the limit of fast recombination and high β values, there is a good correspondence between the asymptotic and numerical results. In Fig. 2b the dependence of the flame speed on r is illustrated for $\beta = 1$, while other parameter values are the same as in figure (a). The value of r is changed more than four orders of magnitude
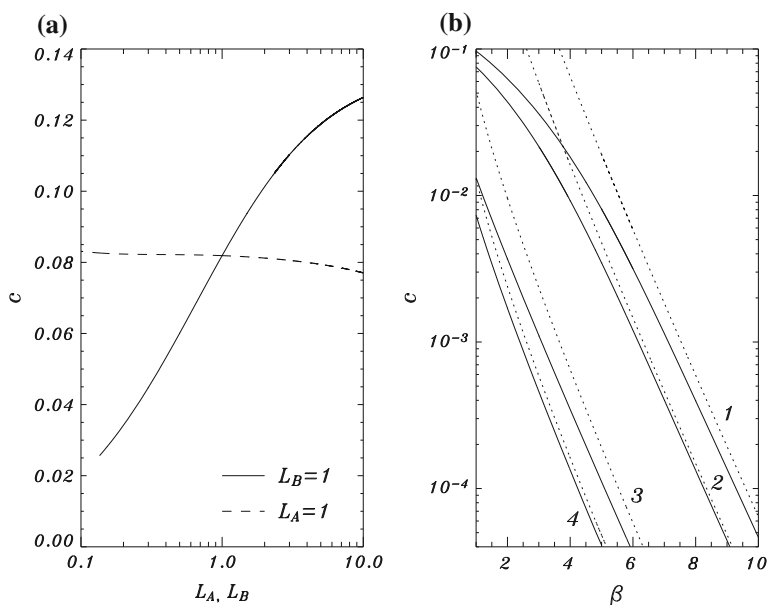
Fig. 3 In figure (**a**) the dependence of the combustion wave speed, c, on L_A for $L_B = 1$ shown with the *solid line* and c on L_B for $L_A = 1$ shown with *dashed line* for $r = \beta = 1$. The Lewis numbers are shown in logarithmic scale. In figure (**b**) the speed is plotted in logarithmic scale as a function of β for $r = 0.01, L_A = 2.0$ curves 1; $r = 0.01, L_A = 0.5$ curves 2; $r = 100, L_A = 2.0$ curves 3; and $r = 100, L_A = 0.5$ curves 4; while $L_B = 1$. The *solid line* represents results from the numerical analysis and the *dotted line* is the solution from the AEA, Eq. (9)

and is plotted in the logarithmic scale in order to show such a variation. There appears a clear maximum in $c(r)$ around $r = 0.1$: for r higher and smaller than this value the combustion wave travels with lower speed. It should be noted that small values of r correspond to slow recombination and large r to fast recombination regime. In other words, there are two trends in $c(r)$ dependence. For slow recombination regime the flame speed increases with r growth and for fast recombination regime $c(r)$ is a monotonically decreasing function.

The results of the analysis of the dependence of the flame speed on the Lewis numbers for fuel and radicals are illustrated in Fig. 3. In (a) the flame speed, c, as a function of L_A is shown with the solid curve for $L_B = 1$ and $c(L_B)$ is shown with the dashed line for $L_A = 1$. The other parameters are taken as $r = \beta = 1$. The Lewis numbers are plotted in logarithmic scale. It is clearly seen that the flame speed is almost not sensitive to the variation of L_B, while it is strongly dependent upon L_A. This result qualitatively correlates with the prediction (9) of the AEA. In Fig. 3b the dependence of $\log c(\beta)$ is plotted for $L_B = 1$ and various values of L_A and r as described in figure caption. The numerical results are shown with the solid line, while the AEA prediction (9) is represented by the dotted lines. Curves 1 ($r = 0.01, L_A = 2.0$) and curves 2 ($r = 0.01, L_A = 0.5$) show good correlation between the asymptotic and numerical results for large values of β. In this case $\log c(\beta)$ becomes almost a linear function and the parameter R is greater than unity indicating that the fast recombination regime

is observed. As β is decreased, the value of R becomes smaller than unity and the fast recombination is replaced with the slow recombination regime. The dependence of $\log c$ on β becomes nonlinear and the correspondence between the numerics and the AEA is poor. For $r = 100.0$ (curves 3 and 4) the fast recombination regime is observed for the whole range of β in Fig. 3b. As a result the numerical and asymptotic results qualitatively agree well for all values of the activation energy considered here.

4 Linear stability

In order to investigate the stability of the combustion waves with respect to the pulsating perturbations we linearize the governing Eq. (5) near the travelling wave solution. In other words, we seek the solution of the form $u(\xi, t) = U(\xi) + \epsilon\phi(\xi)\exp(\lambda t)$, $v(\xi, t) = V(\xi) + \epsilon\psi(\xi)\exp(\lambda t)$, and $w(\xi, t) = W(\xi) + \epsilon\chi(\xi)\exp(\lambda t)$, where $[U(\xi), V(\xi), W(\xi)]$ represent the travelling combustion wave and terms proportional to the small parameter ϵ are the linear perturbation terms. Substituting this expansion into (5), leaving terms proportional to the first order of ϵ only, and introducing the vector function with components $\mathbf{v}(\xi) = [\phi, \psi, \chi, \phi_\xi, \psi_\xi, \chi_\xi]^T$ we obtain

$$\mathbf{v}_\xi = \hat{A}(\xi, \lambda)\mathbf{v}, \tag{10}$$

where

$$\hat{A} = \begin{bmatrix} 0 & \hat{I} \\ \hat{H}(\xi, \lambda) & \hat{C} \end{bmatrix}, \tag{11}$$

$$\hat{H} = \begin{bmatrix} \lambda & 0 & -2rW \\ \beta L_A \frac{VW}{U^2}e^{-1/U} & \beta L_A We^{-1/U} + L_A\lambda & \beta L_A Ve^{-1/U} \\ -\beta L_B \frac{VW}{U^2}e^{-1/U} & -\beta L_B We^{-1/U} & -L_B(\beta Ve^{-1/U} - \lambda - 2\beta rW) \end{bmatrix}, \tag{12}$$

$$\hat{C} = \begin{bmatrix} -c & 0 & 0 \\ 0 & -cL_A & 0 \\ 0 & 0 & -cL_B \end{bmatrix}, \quad \hat{I} = \begin{bmatrix} 1 & 0 & 0 \\ 0 & 1 & 0 \\ 0 & 0 & 1 \end{bmatrix}. \tag{13}$$

We will call a set, Σ, of all λ values for which there exist a solution to (10) bounded for both $\xi \to \pm\infty$ a spectrum of linear perturbations. In the general case, Σ is a set on the complex plane and it consists of the essential spectrum Σ_{ess} and the discrete spectrum Σ_{disc}. If there exists at least one $\lambda \in \Sigma$ such that $\mathrm{Re}\lambda > 0$ then the travelling wave solution is linearly unstable, otherwise, if for all $\lambda \in \Sigma$ the real parts are not positive, then the travelling wave solution is linearly stable. Therefore in order to investigate the linear stability of the travelling wave solutions to (5), the spectrum Σ of the problem (10) has to be found. It can be shown (see [19] for details) that the essential spectrum is comprised of parabolic curves on a complex plane with $\mathrm{Re}\lambda \leq 0$. This implies that

it is the discrete spectrum of the problem (10) that is responsible for the emergence of instabilities.

The linear stability problem is solved by finding the location of the discrete spectrum on the complex plane using the Evans function method [19] implemented with the use of a compound matrix approach (see [16] for more details). The application of the Evans function method to the stability analysis allows one to obtain the location of the discrete spectrum on the complex plane and thus gives detailed information about pulsating instabilities emerging as a result of the loss of stability of the travelling combustion wave. According to [19] the problem of locating points of the discrete spectrum is equivalent to the problem of finding zeros of the Evans function, $E(\lambda)$, on the complex plane. For given set of control parameters L_A, L_B, β, and r we calculate the travelling combustion wave profiles $[U(\xi), V(\xi), W(\xi)]$ as well as the flame speed, c, by solving (7)–(8) numerically. These results are used to formulate the linear stability problem (10) and to calculate the Evans function numerically for some fixed values of λ. By employing the Nyquist plot technique we are able to calculate the number of points of the discrete spectrum located in the right half plane for given set of control parameters and then we locate these points by finding the roots of equation $E(\lambda) = 0$. For small values of activation energy the number of points of the discrete spectrum with $\text{Re}\lambda > 0$ are found to be zero indicating that the travelling combustion wave is stable. As β is increased we reiterate the whole algorithm as described above and at certain value of the activation energy we find that a pair of complex conjugate points of the discrete spectrum moves from the left to the right half of the complex plane crossing the imaginary axis at non-zero values of $\text{Im}\lambda$ i.e. the travelling combustion wave loses stability due to the Hopf bifurcation. These points of the discrete spectrum give rise to pulsating instabilities which can be characterized by the Hopf frequency $\omega = \text{Im}\lambda$. The numerical scheme is then applied repeatedly to analyse the stability of combustion wave for various values of control parameters. The results of our analysis are summarized in Fig. 4a, where the stability diagram is plotted in the L_A vs β plane for $L_B = 1$ and various values of r as described in figure caption. For large L_A, the neutral stability boundary tends to constant values of activation energy. In contrast, as $L_A \to 1$ the combustion wave becomes stable with respect to pulsations or longitudinal perturbations for a wide range of β values i.e. the stability boundary moves towards large values of β. As seen in figure (a) the decrease of r stabilizes the combustion wave solution so that the stability boundary shifts to larger values of the activation energy. As $r \to 1$ and for $r > 1$ the stability boundary in the L_A vs β diagram tends to some limiting behaviour: changing r in two orders of magnitude from 1 to 100 has only weak effect upon stability boundary. In Fig. 4b the Hopf frequency, ω, in logarithmic scale is plotted as a function of β. Almost an exponential decay of ω is observed with an increase of β. The Hopf frequency is also very sensitive to the variation of r. As r is decreased, substantial growth in the frequency of pulsating instabilities is observed. The effect of L_B variation on the stability of the combustion waves is also investigated. It is found that the variation of L_B from 0.3 to 3.0 results in about 1% shift of the stability boundary towards smaller values of β for $r = 1$. Since L_B has only minor influence on the flame stability, the corresponding dependence of L_A on β for critical parameter values is not plotted here.
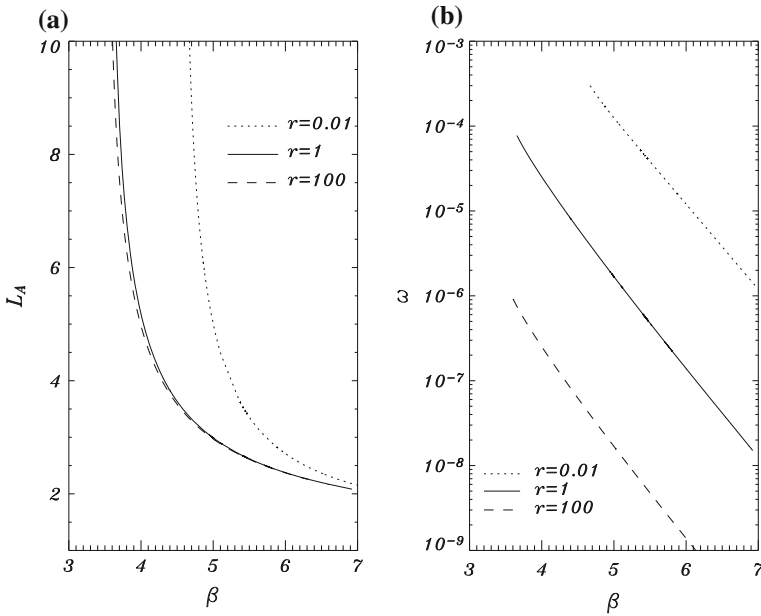
Fig. 4 (**a**) Stability diagram in the L_A versus β parameter plane and (**b**) Hopf frequency in logarithmic scale as function of β. $L_B = 1$ and $r = 100.0$, $r = 1.0$, and $r = 0.01$ are shown with the *dashed*, *solid*, and *dotted lines*, respectively

5 Pulsating solutions and Hopf bifurcation

We investigate the properties of the pulsating combustion wave solutions emerging as a result of the Hopf bifurcation when the parameters reach critical values. The governing equations (5) are solved in a sufficiently large coordinate domain with the boundary conditions (6) imposed at the edge points of the space grid. For our numerical algorithm we use the method of splitting with respect to the physical processes. Initially we solve the set of ordinary differential equations which describe the temperature and the species concentration variations due to the branching and recombination reactions by using the fourth order Runge–Kutta algorithm. As a next step, equations of heat and mass transfer for fuel and radicals are solved with the Crank–Nicholson method of the second-order approximation in space and time. The initial conditions for the numerical scheme are taken in a form of the traveling wave solution (or autowave) of (7).

The results of our investigation are presented in Fig. 5a, b, where the behavior of pulsating combustion wave is illustrated for $L_A = 10$, $L_B = 1$, $r = 1$ and $\beta = 3.8$. The value of β is taken above the critical value of the dimensionless activation energy for the Hopf bifurcation, $\beta_h = 3.657\ldots$ The initial profile taken in the form of the traveling combustion wave is unstable and exhibits pulsating instabilities. These instabilities distort the solutions of (5) at the initial stages of the profile evolution in time. There are transient peaks in the temperature distribution in the coordinate space and oscillations of the shape and maximum value of the radical concentration profile, $w_{\max}$,
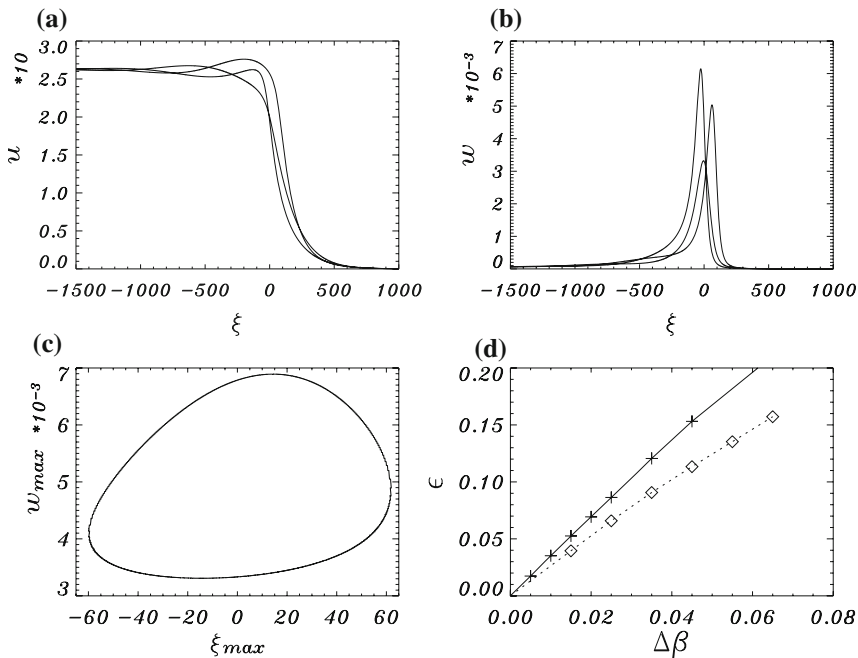
Fig. 5 Pulsating combustion wave solutions for $L_B = 1$, and $r = 1$. In (**a**) and (**b**) the temperature and radical concentration profiles, $u(\xi)$ and $v(\xi)$, are plotted. The profiles are sampled at $t_1 = 0$, $t_2 = 26450$, and $t_3 = 88225$. In (**c**) the limit cycle in the coordinates w_{max} vs. ξ_{max} is shown. In (**a**), (**b**) and (**c**) the activation energy $\beta = 3.8$ and $L_A = 10$. In (**d**) the relative square amplitude, ϵ, is plotted as a function of the bifurcation parameter, $\Delta\beta$ for $L_A = 10$ shown with the *crosses* connected with the *solid line* and for $L_A = 3$ shown with the *diamonds* connected with the *dotted line*

are observed. The fuel concentration profile is mainly affected in the variation of the front curvature although some small oscillations of the fuel concentration are observed in the product region. The value of w_{max} and the location of the maximum of the radical concentration ξ_{max} are convenient parameters to describe the pulsating nature of the solution. Here $\xi = x - c_{drift}t$ is a coordinate in the frame traveling with speed c_{drift} which is a mean value of the flame propagation velocity $c_{drift} = \lim_{t \to} x_{max}/t$, where x_{max} is a coordinate of the maximum of the radical concentration in the laboratory coordinate frame. As the pulsating instabilities evolve, the value of w_{max} and ξ_{max} oscillate with an amplitude which initially grows exponentially with time. The frequency of these oscillations is given by the imaginary part $\text{Im}\lambda$ and the rate of exponential growth is determined by the real part, $\text{Re}\lambda$, of the pair of points of the discrete spectrum, responsible for the onset of instability. At times of the order of $(\text{Re}\lambda)^{-1}$, the amplitudes of oscillations, w_{max} and ξ_{max}, reach saturation and stabilize at certain values. The behavior of $u(\xi, t)$, $v(\xi, t)$, and $w(\xi, t)$ profiles become periodic in time and so the pulsating combustion wave is formed. In Fig. 5a and b the temperature and the concentration of radicals profiles of the pulsating combustion wave are plotted respectively for three moments of time $t_1 = 0$, $t_2 = 26450$, and $t_3 = 88225$. Since the solution is periodic, time is measured from 0 to T, where $T = 111800$ is the period

of oscillations. For the temperature profile, Fig. 5a, there are local peaks of temperature, which oscillate in time. Also we note that the value of ξ_{max} of the temperature maximum as well as the coordinate of the maximum slope of $u(\xi)$ oscillates in time near $\xi = 0$. The fuel concentration profile $v(\xi, t)$ is not plotted here. However, we note that the maximum slope of $v(\xi)$ for fixed t changes its value with time and also the coordinate of the maximum slope exhibits oscillations over a period of time near the origin $\xi = 0$. The most remarkable soliton type dynamics is demonstrated by the radical concentration profile $w(\xi, t)$, which is depicted in Fig. 5b. As seen from this figure the radical concentration as a function of ξ remains a bell-shaped function of the soliton type for all moments of time. However, the maximum of $w(\xi)$ and its location are periodic functions of time. This is demonstrated in Fig. 5c, where w_{max} is plotted versus ξ_{max}. It is seen that a limit cycle is formed in the (ξ_{max}, w_{max}) plane.

In order to clarify the nature of the Hopf bifurcation, the properties of the pulsating solutions emerging from the traveling combustion wave have been investigated. The results of this investigation are presented in Fig. 5d, where calculations have been undertaken for $L_A = 3.0$ and $L_A = 10$. Other parameters are taken as shown in figure caption. Parameter β is increased from the values just above the critical value for the Hopf bifurcation β_h and the pulsating combustion wave is found by solving (5) for each β. In Fig. 5d the relative square amplitude, $\epsilon = \Delta w_{max}^2 / w_h^2$, is plotted against the critical parameter $\Delta\beta = \beta - \beta_h$, where $\Delta w_{max} = \max\{w_{max}(t)\} - \min\{w_{max}(t)\}$ over one period $0 < t < T$, w_h is the maximum of the radical concentration for the travelling combustion wave taken at the Hopf bifurcation, $\beta = \beta_h$. Crosses connected with the solid line correspond to $L_A = 10$ and diamonds connected with the dashed line represent $L_A = 3$. For small values of critical parameter $\Delta\beta$, just beyond the the neutral stability boundary, the squared amplitude shows a linear behaviour. The amplitude of oscillations is continuous and root-type function of $\Delta\beta$. This is typical for supercritical Hopf bifurcation from which stable periodic solutions emanate giving rise to stable limit cycles. As $\Delta\beta$ is increased the dependence of ϵ on $\Delta\beta$ becomes nonlinear. The dependence of ϵ on β allows us to obtain the critical parameter values for the Hopf bifurcation by the linear fit of the data of the direct integration of the governing equations (5). These values are found to agree with the results of the linear stability analysis up to the third significant digit, confirming the validity of both approaches.

6 Conclusions

In this paper the properties and the stability of combustion waves in the one-dimensional Zeldovich–Liñán model is considered in the adiabatic limit. The structure of the travelling combustion wave is found to depend on the recombination parameter, R, showing the relation between the characteristic times of the branching and recombination reactions. For small values of R, the slow recombination regime of flame propagation is observed. In this case the leading edge of the flame is governed by heat and species diffusion, the reaction zone consists of the thin branching zone embedded into much wider recombination region. In the branching zone almost all fuel is converted to radicals and the radical concentration reaches the values of the order of $O(1)$. In the recombination region the radicals are transformed into the products and heat is released. The recombination reaction spreads to the product zone, where the

recombination, rather than the transport effects are dominating. As a result the temperature and species concentrations approach the asymptotic values in sub-exponential manner. In the case of large R, the recombination reaction is faster than branching reaction and the fast recombination regime of flame propagation is observed. In the upstream region the transport effects are dominating. This preheat zone is followed by the reaction region, where the recombination reaction follows the branching reaction and a steady-state approximation applies to the radical species. As a result, the radical concentration is small. The two-step reaction model can be reduced to the one-step reaction model with second-order reaction and double the activation energy of that for the branching reaction in the two-step model. The results of the AEA analysis for the one-step model are compared to the numerical data obtained for the Zeldovich–Liñán model. It is found that the correspondence is good for the fast recombination regime and large activation energies. In the slow recombination regime the discrepancy between the one-step and two-step models is substantial.

The properties of the combustion wave are investigated in detail by the use of numerical integration. It is found that the flame speed is unique, the combustion wave does not exhibit extinction as the activation energy is increased in contrast to the model with the first order recombination reaction [14]. The flame speed is a monotonically decreasing function of the activation energy. The variation of L_A effects the properties of combustion wave substantially, so that the combustion wave travels faster for larger values of L_A. In contrast, the variation of L_B has almost no effect on the flame speed. The influence of r on the speed of combustion wave is different for various flame regimes: in the fast recombination regime $c(r)$ is monotonically decreasing and in the slow recombination regime $c(r)$ is monotonically increasing function. The latter contradicts with the prediction (9) of the one-step AEA analysis.

The stability of combustion waves with respect to pulsating perturbations was investigated by using the Evans function method and by direct integration of the governing partial-differential equations. The results from both methods are found to agree with high degree of accuracy. It was determined that the travelling combustion wave loses stability due to the Hopf bifurcation. As the bifurcation parameter is varied, a pair of complex conjugate points of the discrete spectrum of the linear stability problem moves from the left to the right half of the complex plane crossing the imaginary axis at nonzero coordinates giving rise to pulsating instabilities. The critical parameter values for the Hopf bifurcation were found. It was demonstrated that on the L_A versus β plane the neutral stability boundary $L_A(\beta)$ is a monotonically decaying function. For large values of the Lewis number for fuel the critical activation energy for the Hopf bifurcation, β_h, tends to a definite constant value, whereas for $L_A \to 1$ the travelling combustion wave becomes stable with respect to pulsating perturbations i.e. $\beta_h \to \infty$. Varying the Lewis number for radicals, L_B, has only weak quantitative effect on the stability of combustion waves. On the other hand the influence of r depends on the specific flame regime. For large r in the case of fast recombination, the stability of combustion waves is almost independent of r, for example, the increase of r in two orders of magnitude from 1 to 100 only slightly shifts the neutral stability boundary towards smaller values of β. In contrast, for small values of r in the slow recombination regime, the stability of the combustion wave becomes very sensitive to variation of r. For fixed r in the case of small and moderate activation energies so that $R < 1$,

the combustion wave becomes stable i.e. the flame is stable in the slow recombination regime. The neutral stability boundary shifts to large β values such that $R > 1$ i.e. to the parameter region corresponding to the fast recombination regime. In other words, decreasing r below unity has a stabilizing effect on combustion wave. The nature of the Hopf bifurcation and the properties of the pulsating solutions emerging as a result of this bifurcation were investigated. It is demonstrated that the Hopf bifurcation is supercritical. The amplitude of pulsations grow in a root type manner as the activation energy is increased beyond the neutral stability boundary.

It is not clear at the moment if any further increase of bifurcation parameter would result in a sequence of period doubling and chaos [16]. The clarification of this issue is the subject of our future work. However, at this stage of investigation it is clear that the kinetics of the recombination reaction has a strong influence on both the properties and stability of combustion waves.

Finally we would like to point out that our current study of the combustion waves in the Zeldovich–Liñán model, which possesses second-order recombination reaction, has properties that are more common to the adiabatic one-step models. This is in contrast to the first-order recombination reaction studies in [13–16]. In the latter model, the existence of combustion wave extinction and the presence of the Bogdanov–Takens bifurcation point is demonstrated even for the adiabatic case. Similar behaviour can be expected [4] for the nonadiabatic Zeldovich–Liñán model and the clarification of this issue is also the subject of our future investigation.

Appendix

The leading order asymptotic behaviour for $\xi \to -\infty$ of the solution to the system of Eq. (7) can be found by introducing new independent variable $z = w$ and new dynamical variables $y \equiv u$, $q \equiv v$, $p \equiv dw/d\xi$. We can rewrite (7) as

$$
\begin{aligned}
p^2 y_{zz} + pp_z y_z + cpy_z + rz^2 &= 0, \\
L_A^{-1}(p^2 q_{zz} + pp_z q_z) + cpq_z - \beta z q e^{-1/y} &= 0, \\
L_B^{-1} pp_z + cp + \beta z q e^{-1/y} - r\beta z^2 &= 0.
\end{aligned}
\tag{14}
$$

We seek bounded solution to (14), which satisfies the following conditions: $p(0) = 0$, since the derivative $dw/d\xi$ vanishes as $\xi \to -\infty$ or $z \to 0$; we require that $w(\xi)$ approaches zero monotonically and therefore $p(z) > 0$ for sufficiently small z values. The solution is represented in a form of a series

$$
y(z) = y_0 + y_1 z + \cdots, \qquad q(z) = q_0 + q_1 z + \cdots, \qquad p(z) = p_1 z + \cdots. \tag{15}
$$

with z being a small parameter of asymptotic expansion. Substituting (15) into (14) we obtain in the first order $O(z)$:

$$y_1(p_1^2 + cp_1) = 0, \qquad L_A^{-1}p_1^2 q_1 + cp_1 q_1 - \beta q_0 e^{-1/y_0} = 0,$$
$$L_B^{-1}p_1^2 + cp_1 + \beta q_0 e^{-1/y_0} = 0. \tag{16}$$

The last equation in (16) gives two solutions $p_1 = L_B\left(-c \pm \sqrt{c^2 - 4\beta L_B^{-1} q_0 e^{-1/y_0)}}\right)/2$, which are both negative if $q_0 > 0$. If negative p_1 is taken, it implies that $p(z) < 0$ for some sufficiently small z values, which contradicts the requirement that $w(\xi)$ is monotonic. Thus the trivial solution $q_0 = 0$ and $p_1 = 0$ is chosen to aviod the contradiction. Taking this into account we write the second-order equations as

$$cp_2 y_1 + r = 0, \quad cp_2 q_1 - \beta q_1 e^{-1/y_0} = 0, \quad cp_2 + \beta q_1 e^{-1/y_0} - \beta r = 0, \tag{17}$$

which yield two solutions $p_2 = \beta e^{-1/u_0}/c, q_1 = re^{1/y_0} - 1, y_1 = -re^{1/y_0}/\beta$ and $p_2 = \beta r/c, q_1 = 0, y_1 = -\beta^{-1}$. The first solution is valid for $re^{-1/y_0} > 1$ and the second for $re^{-1/y_0} < 1$.

Returning to original variables we obtain that $q_0 = 0$ implies $\sigma = 0$ and so $y_0 = \beta^{-1}$. The asymptotic relation between the dynamical variables valid in the limit $\xi \to -\infty$ can be written as

$$u = (1 - re^{\beta}w)/\beta, \quad v = (re^{\beta} - 1)w, \quad w_\xi = \beta e^{-\beta}/cw^2 \text{ for } re^{\beta} > 1,$$
$$u = (1 - w)/\beta, \qquad v = 0, \qquad w_\xi = \beta r/cw^2 \quad \text{for } re^{\beta} < 1, \tag{18}$$

References

1. Y.B. Zeldovich, Zh. Phys. Khim. **22**, 27 (1948), English translation in NACA TM 1282 (1951)
2. A. Liñán, Insituto Nacional de Technica Aerospacial "Esteban Terradas" (Madrid), USAFOSR Contract No. E00AR68-0031, Technical Report No. 1 (1971)
3. G. Joulin, A. Liñán, G.S.S. Ludford, N. Peters, C. Schmidt-Lainé, SIAM J. Appl. Math. **45**, 420 (1985)
4. B.H. Chao, C.K. Law, Int. J. Heat Mass Transfer **37**, 673 (1994)
5. G. Joulin, P. Clavin, Combust. Flame **35**, 139 (1979)
6. K. Seshardi, N. Peters, Combust. Sci. Tech. **33**, 35 (1983)
7. D.W. Mikolaitis, Combust. Sci. Tech. **49**, 277 (1986)
8. R.Y. Tam, Combust. Sci. Tech. **60**, 125 (1988)
9. R.Y. Tam, Combust. Sci. Tech. **62**, 297 (1988)
10. Y.B. Zeldovich, Kinet. Katal. **11**, 305 (1961)
11. D. Fernandez-Galisteo, Gonzalo del Alamo, A.L. Sanchez, A. Linan, in *Proceedings of the Third European Combustion Meeting*, Paper 6–19, 1–5 (2007)
12. O.P. Korobeinichev, T.A. Bol'shova, Comb. Expl. Shock Waves **45**, 507 (2009)
13. J.W. Dold, Combust. Theory Mod. **11**, 909 (2007)
14. V.V. Gubernov, H.S. Sidhu, G.N. Mercer, Combust. Theory Mod. **12**, 407 (2008)
15. V.V. Gubernov, H.S. Sidhu, G.N. Mercer, A.V. Kolobov, A.A. Polezhaev, J. Math. Chem. **44**, 816 (2008)
16. V.V. Gubernov, H.S. Sidhu, G.N. Mercer, A.V. Kolobov, A.A. Polezhaev, Int. J. Bif. Chaos **19**, 873 (2009)
17. R.O. Weber, G.N. Mercer, H.S. Sidhu, B.F. Gray, Proc. R. Soc. A **453**, 1105 (1997)
18. A.I. Volpert, V.A. Volpert, V.A. Volpert, *Traveling Wave Solutions of Parabolic Systems* (American Mathematical Society, Providence, Rhode Island, 1991).
19. B. Sandstede, in, ed. by B. Fiedler Handbook of Dynamical Systems II (Elsevier, North-Holland, 2002), pp. 983–1055